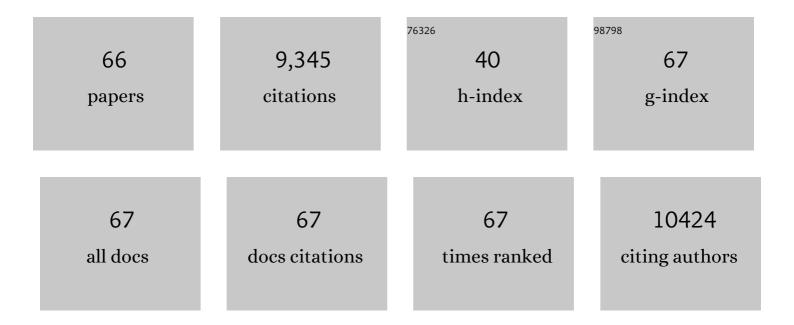
List of Publications by Year in descending order

Source: https://exaly.com/author-pdf/3693965/publications.pdf

Version: 2024-02-01



**ГІЗНА 7НАМС** 

#	Article	IF	CITATIONS
1	Semiconductor heterojunction photocatalysts: design, construction, and photocatalytic performances. Chemical Society Reviews, 2014, 43, 5234.	38.1	3,257
2	Bi <sub>2</sub> WO <sub>6</sub> Nano―and Microstructures: Shape Control and Associated Visibleâ€Lightâ€Driven Photocatalytic Activities. Small, 2007, 3, 1618-1625.	10.0	566
3	Fabrication of flower-like Bi2WO6 superstructures as high performance visible-light driven photocatalysts. Journal of Materials Chemistry, 2007, 17, 2526.	6.7	439
4	Ultrathin PEGylated W <sub>18</sub> O <sub>49</sub> Nanowires as a New 980 nm‣aserâ€Driven Photothermal Agent for Efficient Ablation of Cancer Cells In Vivo. Advanced Materials, 2013, 25, 2095-2100.	21.0	370
5	Sonochemical synthesis of nanocrystallite Bi2O3 as a visible-light-driven photocatalyst. Applied Catalysis A: General, 2006, 308, 105-110.	4.3	356
6	A sonochemical route to visible-light-driven high-activity BiVO4 photocatalyst. Journal of Molecular Catalysis A, 2006, 252, 120-124.	4.8	340
7	AgBr-Ag-Bi2WO6 nanojunction system: A novel and efficient photocatalyst with double visible-light active components. Applied Catalysis A: General, 2009, 363, 221-229.	4.3	304
8	Single-Crystalline BiVO <sub>4</sub> Microtubes with Square Cross-Sections:  Microstructure, Growth Mechanism, and Photocatalytic Property. Journal of Physical Chemistry C, 2007, 111, 13659-13664.	3.1	247
9	Fabrication of g-C3N4/BiOBr heterojunctions on carbon fibers as weaveable photocatalyst for degrading tetracycline hydrochloride under visible light. Chemical Engineering Journal, 2020, 386, 124010.	12.7	231
10	Ultrasonic-assisted synthesis of visible-light-induced Bi2MO6 (M=W, Mo) photocatalysts. Journal of Molecular Catalysis A, 2007, 268, 195-200.	4.8	184
11	Synthesis of Ta <sub>3</sub> N <sub>5</sub> /Bi <sub>2</sub> MoO <sub>6</sub> core–shell fiber-shaped heterojunctions as efficient and easily recyclable photocatalysts. Environmental Science: Nano, 2017, 4, 1155-1167.	4.3	180
12	Electrodeposited nanoporous ZnO films exhibiting enhanced performance in dye-sensitized solar cells. Electrochimica Acta, 2006, 51, 5870-5875.	5.2	146
13	Growth of C3N4 nanosheets on carbon-fiber cloth as flexible and macroscale filter-membrane-shaped photocatalyst for degrading the flowing wastewater. Applied Catalysis B: Environmental, 2017, 219, 425-431.	20.2	132
14	TiO2/BiOI p-n junction-decorated carbon fibers as weavable photocatalyst with UV–vis photoresponsive for efficiently degrading various pollutants. Chemical Engineering Journal, 2021, 415, 129019.	12.7	130
15	Construction of n-TiO2/p-Ag2O Junction on Carbon Fiber Cloth with Vis–NIR Photoresponse as a Filter-Membrane-Shaped Photocatalyst. Advanced Fiber Materials, 2020, 2, 13-23.	16.1	126
16	Bi2WO6 micro/nano-structures: Synthesis, modifications and visible-light-driven photocatalytic applications. Applied Catalysis B: Environmental, 2011, 106, 1-1.	20.2	110
17	Visible-light-driven photocatalytic inactivation of Escherichia coli by magnetic Fe2O3–AgBr. Water Research, 2016, 90, 111-118.	11.3	106
18	Synthesis of BiOBr/WO <sub>3</sub> p–n heterojunctions with enhanced visible light photocatalytic activity. CrystEngComm, 2016, 18, 3856-3865.	2.6	104

#	Article	IF	CITATIONS
19	Preparation of Fenton reagent with H2O2 generated by solar light-illuminated nano-Cu2O/MWNTs composites. Applied Catalysis A: General, 2006, 299, 292-297.	4.3	95
20	High Efficiency CdS/CdSe Quantum Dot Sensitized Solar Cells with Two ZnSe Layers. ACS Applied Materials & Interfaces, 2016, 8, 34482-34489.	8.0	85
21	Preparation of TiO2/C3N4 heterojunctions on carbon-fiber cloth as efficient filter-membrane-shaped photocatalyst for removing various pollutants from the flowing wastewater. Journal of Colloid and Interface Science, 2018, 532, 798-807.	9.4	85
22	Synthesis of flower-like Ag2O/BiOCOOH p-n heterojunction with enhanced visible light photocatalytic activity. Applied Surface Science, 2017, 397, 95-103.	6.1	81
23	Synthesis of Au nanoparticle-decorated carbon nitride nanorods with plasmon-enhanced photoabsorption and photocatalytic activity for removing various pollutants from water. Journal of Hazardous Materials, 2018, 344, 1188-1197.	12.4	81
24	Preparation of TiO <sub>2</sub> /Bi <sub>2</sub> WO <sub>6</sub> nanostructured heterojunctions on carbon fibers as a weaveable visible-light photocatalyst/photoelectrode. Environmental Science: Nano, 2018, 5, 327-337.	4.3	80
25	Electrodeposition and characterization of nanocrystalline cuprous oxide thin films on TiO2 films. Materials Letters, 2005, 59, 434-438.	2.6	78
26	Flower-like Bi <sub>2</sub> S <sub>3</sub> /Bi <sub>2</sub> MoO <sub>6</sub> heterojunction superstructures with enhanced visible-light-driven photocatalytic activity. RSC Advances, 2015, 5, 75081-75088.	3.6	78
27	980â€nm Laserâ€Driven Photovoltaic Cells Based on Rareâ€Earth Upâ€Converting Phosphors for Biomedical Applications. Advanced Functional Materials, 2009, 19, 3815-3820.	14.9	75
28	Surface decoration of Bi2WO6 superstructures with Bi2O3 nanoparticles: an efficient method to improve visible-light-driven photocatalytic activity. CrystEngComm, 2013, 15, 9011.	2.6	75
29	Low temperature cathodic electrodeposition of nanocrystalline zinc oxide thin films. Thin Solid Films, 2005, 492, 24-29.	1.8	63
30	Synthesis of ZnWO4â^'x nanorods with oxygen vacancy for efficient photocatalytic degradation of tetracycline. Progress in Natural Science: Materials International, 2018, 28, 408-415.	4.4	61
31	TiO2/MoS2 heterojunctions-decorated carbon fibers with broad-spectrum response as weaveable photocatalyst/photoelectrode. Materials Research Bulletin, 2019, 112, 354-362.	5.2	53
32	Ta3N5-Pt nonwoven cloth with hierarchical nanopores as efficient and easily recyclable macroscale photocatalysts. Scientific Reports, 2014, 4, 3978.	3.3	52
33	MIL-101(Fe) nanodot-induced improvement of adsorption and photocatalytic activity of carbon fiber/TiO2-based weavable photocatalyst for removing pharmaceutical pollutants. Journal of Cleaner Production, 2021, 290, 125782.	9.3	52
34	MoS2/Bi2S3 heterojunctions-decorated carbon-fiber cloth as flexible and filter-membrane-shaped photocatalyst for the efficient degradation of flowing wastewater. Journal of Alloys and Compounds, 2019, 779, 599-608.	5.5	51
35	Construction of TiO2/Ag3PO4 nanojunctions on carbon fiber cloth for photocatalytically removing various organic pollutants in static or flowing wastewater. Journal of Colloid and Interface Science, 2020, 571, 213-221.	9.4	50
36	Synthesis of MoS <sub>2</sub> /CdS Heterostructures on Carbonâ€Fiber Cloth as Filterâ€Membraneâ€Shaped Photocatalyst for Purifying the Flowing Wastewater under Visibleâ€Light Illumination. ChemCatChem, 2019, 11, 2855-2863.	3.7	49

#	Article	IF	CITATIONS
37	Synthesis of BiOBr/Ag3PO4 heterojunctions on carbon-fiber cloth as filter-membrane-shaped photocatalyst for treating the flowing antibiotic wastewater. Journal of Colloid and Interface Science, 2020, 575, 183-193.	9.4	49
38	Fabrication of MoS <sub>2</sub> /BiOBr heterojunctions on carbon fibers as a weaveable photocatalyst for tetracycline hydrochloride degradation and Cr( <scp>vi</scp> ) reduction under visible light. Environmental Science: Nano, 2020, 7, 2708-2722.	4.3	47
39	Synthesis of polypyrrole nanoparticles for constructing full-polymer UV/NIR-shielding film. RSC Advances, 2015, 5, 96888-96895.	3.6	46
40	BiOBr/Ag/AgBr heterojunctions decorated carbon fiber cloth with broad-spectral photoresponse as filter-membrane-shaped photocatalyst for the efficient purification of flowing wastewater. Journal of Colloid and Interface Science, 2021, 587, 633-643.	9.4	45
41	Fabrication of NH2-MIL-125(Ti) nanodots on carbon fiber/MoS2-based weavable photocatalysts for boosting the adsorption and photocatalytic performance. Journal of Colloid and Interface Science, 2022, 611, 706-717.	9.4	43
42	Construction of C3N4/CdS nanojunctions on carbon fiber cloth as a filter-membrane-shaped photocatalyst for degrading flowing wastewater. Journal of Alloys and Compounds, 2021, 851, 156743.	5.5	40
43	Construction of titanium dioxide/cadmium sulfide heterojunction on carbon fibers as weavable photocatalyst for eliminating various contaminants. Journal of Colloid and Interface Science, 2020, 561, 307-317.	9.4	39
44	Visâ€NIR Lightâ€Responsive Photocatalytic Activity of C <sub>3</sub> N <sub>4</sub> â^'Agâ^'Ag <sub>2</sub> O Heterojunctionâ€Decorated Carbonâ€fiber Cloth as Efficient Filterâ€Membraneâ€Shaped Photocatalyst. ChemCatChem, 2019, 11, 1362-1373.	3.7	38
45	Boosting the adsorption and photocatalytic activity of carbon fiber/MoS2-based weavable photocatalyst by decorating UiO-66-NH2 nanoparticles. Chemical Engineering Journal, 2021, 417, 128112.	12.7	38
46	Synthesis of Yb 3+ /Er 3+ co-doped Bi 2 WO 6 nanosheets with enhanced photocatalytic activity. Materials Letters, 2016, 163, 16-19.	2.6	36
47	Fe2O3–AgBr nonwoven cloth with hierarchical nanostructures as efficient and easily recyclable macroscale photocatalysts. RSC Advances, 2015, 5, 10951-10959.	3.6	34
48	Hydrothermal synthesis of graphene/TiO 2 /CdS nanocomposites as efficient visible-light-driven photocatalysts. Materials Letters, 2017, 194, 172-175.	2.6	31
49	Construction of Ag/AgCl-CN heterojunctions with enhanced photocatalytic activities for degrading contaminants in wastewater. Journal of Colloid and Interface Science, 2019, 543, 25-33.	9.4	31
50	Growth of TiO <sub>2</sub> nanorod bundles on carbon fibers as flexible and weaveable photocatalyst/photoelectrode. RSC Advances, 2015, 5, 102868-102876.	3.6	27
51	Construction of 980 nm laser-driven dye-sensitized photovoltaic cell with excellent performance for powering nanobiodevices implanted under the skin. Journal of Materials Chemistry, 2012, 22, 18156.	6.7	26
52	Synthesis of CuS nanoplate-containing PDMS film with excellent near-infrared shielding properties. RSC Advances, 2016, 6, 18881-18890.	3.6	26
53	Synthesis of NiTiO <sub>3</sub> –Bi <sub>2</sub> MoO <sub>6</sub> core–shell fiber-shaped heterojunctions as efficient and easily recyclable photocatalysts. New Journal of Chemistry, 2018, 42, 411-419.	2.8	24
54	Preparation of Yb3+/Er3+ co-doped BiOCl sheets as efficient visible-light-driven photocatalysts. Materials Letters, 2016, 179, 154-157.	2.6	23

#	Article	IF	CITATIONS
55	Flexible fiber-shaped CulnSe2 solar cells with single-wire-structure: Design, construction and performance. Nano Energy, 2012, 1, 769-776.	16.0	21
56	Decoration of amine functionalized zirconium metal organic framework/silver iodide heterojunction on carbon fiber cloth as a filter- membrane-shaped photocatalyst for degrading antibiotics. Journal of Colloid and Interface Science, 2021, 603, 582-593.	9.4	20
57	Bismuth oxybromide/bismuth oxyiodide nanojunctions decorated on flexible carbon fiber cloth as easily recyclable photocatalyst for removing various pollutants from wastewater. Journal of Colloid and Interface Science, 2022, 608, 2660-2671.	9.4	17
58	Facile one-pot sonochemical synthesis of hydrophilic ultrasmall LaF3:Ce,Tb nanoparticles with green luminescence. Progress in Natural Science: Materials International, 2012, 22, 488-492.	4.4	15
59	Simultaneous control of morphology, phase and optical absorption of hydrophilic copper sulfide-based photothermal nanoagents through Cu/S precursor ratios. Journal of Alloys and Compounds, 2015, 648, 98-103.	5.5	15
60	Watermelon Fleshâ€Đerived Carbon Aerogel with Hierarchical Porous Structure for Interfacial Solar Steam Generation. Solar Rrl, 2022, 6, .	5.8	12
61	Synthesis of Cu <sub>2</sub> ZnSnS <sub>4</sub> film by air-stable molecular-precursor ink for constructing thin film solar cells. RSC Advances, 2014, 4, 36046.	3.6	9
62	Growth of Cu <sub>2</sub> O Spherical Superstructures on g-C <sub>3</sub> N <sub>4</sub> as Efficient Visible-Light-Driven <i>p</i> – <i>n</i> Heterojunction Photocatalysts for Degrading Various Organic Pollutants. Journal of Nanoscience and Nanotechnology, 2018, 18, 7355-7363.	0.9	9
63	In situ growth of CulnS2 nanocrystals on nanoporous TiO2 film for constructing inorganic/organic heterojunction solar cells. Nanoscale Research Letters, 2013, 8, 354.	5.7	4
64	Synthesis of flexible and up-converting luminescent NaYF <sub>4</sub> :Yb,Er-PET composite film for constructing 980-nm laser-driven biopower. RSC Advances, 2016, 6, 42763-42769.	3.6	3
65	Synthesis of ultrathin g-C3N4/graphene nanocomposites with excellent visible-light photocatalytic performances. Functional Materials Letters, 2019, 12, 1950025.	1.2	3
66	Synthesis of Cu2(OH)PO4 superstructures with NIR-laser enhanced photocatalytic activity. Functional Materials Letters, 2020, 13, 2050015.	1.2	1